Supporting Information

Thiol Ligand-Induced Transformation of $Au_{38}(SC_2H_4Ph)_{24}$ to $Au_{36}(SPh\text{-}t\text{-}Bu)_{24}$

Chenjie Zeng,[†] Chunyan Liu,[‡] Yong Pei,[‡] and Rongchao Jin[†,*]

[†]*Department of Chemistry, Carnegie Mellon University, 4400 Fifth Ave, Pittsburgh, PA 15213, United States*
[‡]*Department of Chemistry, Key Laboratory of Environmentally Friendly Chemistry and Applications of Ministry of Education, Xiangtan University, Hunan Province 411105, People's Republic of China*

A) Full range ESI-MS spectrum for the 5-min product:

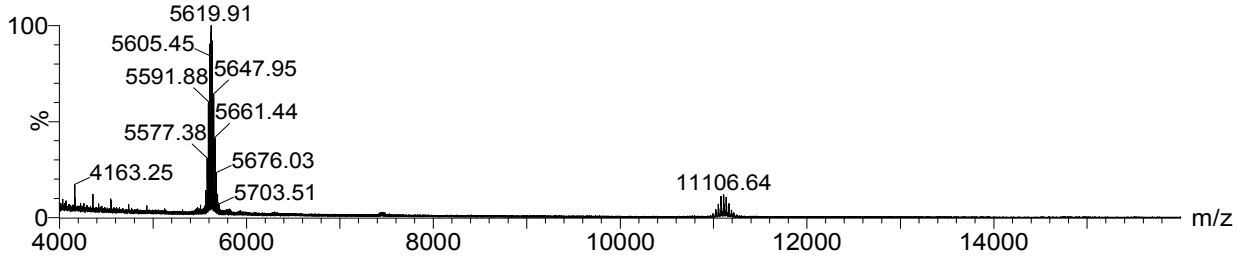

B) Full range ESI-MS spectrum for the 20-min product:

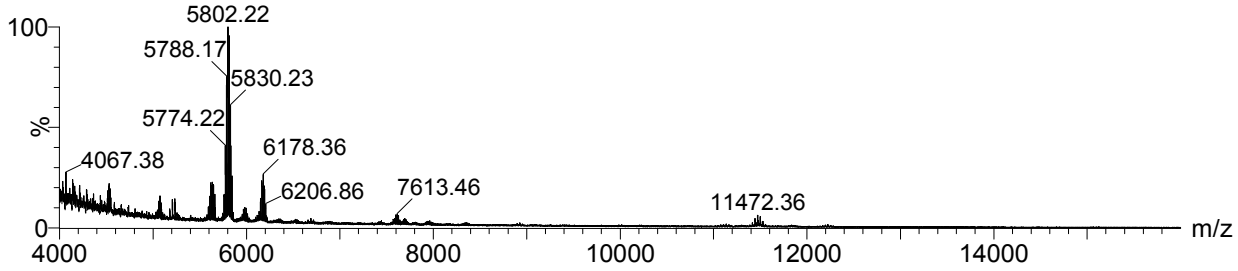

Figure S1. Full range ESI-MS spectra of the intermediate stages, A) initial ligand-exchange (5 min), B) disproportionation stage (e.g. 20 min). In the upper panel: The m/z 5619.91 ion set corresponding to **2+** and m/z 11106.64 to **1+** set. The peak assignment is provided in Table S1. For detail explanation, see main text.

Table S1. Identification of species in ESI-MS spectra at different reaction times. A) to C) corresponding to Au_{38}, Au_{36} and Au_{40}, respectively.

A).

$[Au_{38}(TBBT)_x(PET)_yCs_2]^{2+}$		m/z Cal.	m/z Experiment						
x	y		0 min	5 min	10 min	15 min	20 min	35 min	60min
0	24	5521.68	5521.77						
1	23	5535.71							
2	22	5549.74		5549.68					
3	21	5563.77		5563.85					
4	20	5577.8		5577.46					
5	19	5591.83		5591.80					

6	18	5605.86		5605.91	5605.78				
7	17	5619.89		5619.94	5619.94				
8	16	5633.92		5633.97	5633.92				
9	15	5647.95		5648.00	5647.95				
10	14	5661.98		5661.88	5661.99				
11	13	5676.01		5675.94	5675.97				
12	12	5690.04		5690.08	5689.97	5689.99			
13	11	5704.07		5703.59	5703.98	5704.01			
14	10	5718.10			5718.01	5718.01			
15	9	5732.13			5732.03	5732.00			
16	8	5746.16			5746.10	5746.04			
17	7	5760.19			5760.18	5760.07	5760.26		
18	6	5774.22			5774.03	5774.00	5774.25	5774.08	
19	5	5788.25			5788.20	5788.17	5788.17	5788.14	
20	4	5802.28				5802.2	5802.31	5802.14	5802.12
21	3	5816.31				5816.21	5816.26	5816.18	5816.58
22	2	5830.34				5829.81	5830.23	5830.26	5830.21
23	1	5844.37					5844.28	5844.25	5844.2
24	0	5858.40						5858.42	5858.23

B).

$[\mathbf{Au_{36}}(TBBT)_x(PET)_yCs_2]^{2+}$		m/z cal.	m/z experiment				
x	y		20 min	35 min	60 min	120 min	240 min
16	8	5548.89					
17	7	5562.91					
18	6	5577.25					
19	5	5591.28	5591.25	5591.25			
20	4	5605.31	5605.31	5605.86			
21	3	5619.34	5619.30	5619.24			
22	2	5633.37	5633.34	5633.25	5633.38	5633.28	5633.20
23	1	5647.40	5647.39	5647.28	5647.29	5647.28	5647.20
24	0	5661.43	5661.35	5661.30	5661.28	5661.33	5661.24

C).

$[\mathbf{Au_{40}}(TBBT)_x(PET)_yCs_2]^{2+}$		m/z cal.	m/z experiment				
x	y		20 min	35 min	60 min	120 min	240 min
16	10	6080.32					
17	9	6094.35					
18	8	6108.38					
19	7	6122.41					
20	6	6136.44	6136.56				
21	5	6150.47	6150.31				
22	4	6164.50	6164.47	6164.15			
23	3	6178.53	6178.42	6178.62	6178.71		
24	2	6192.56	6192.82	6192.32	6192.74	6192.21	
25	1	6206.59	6206.86	6206.57	6206.6	6206.36	
26	0	6220.62	6220.74	6220.33	6220.63	6220.77	

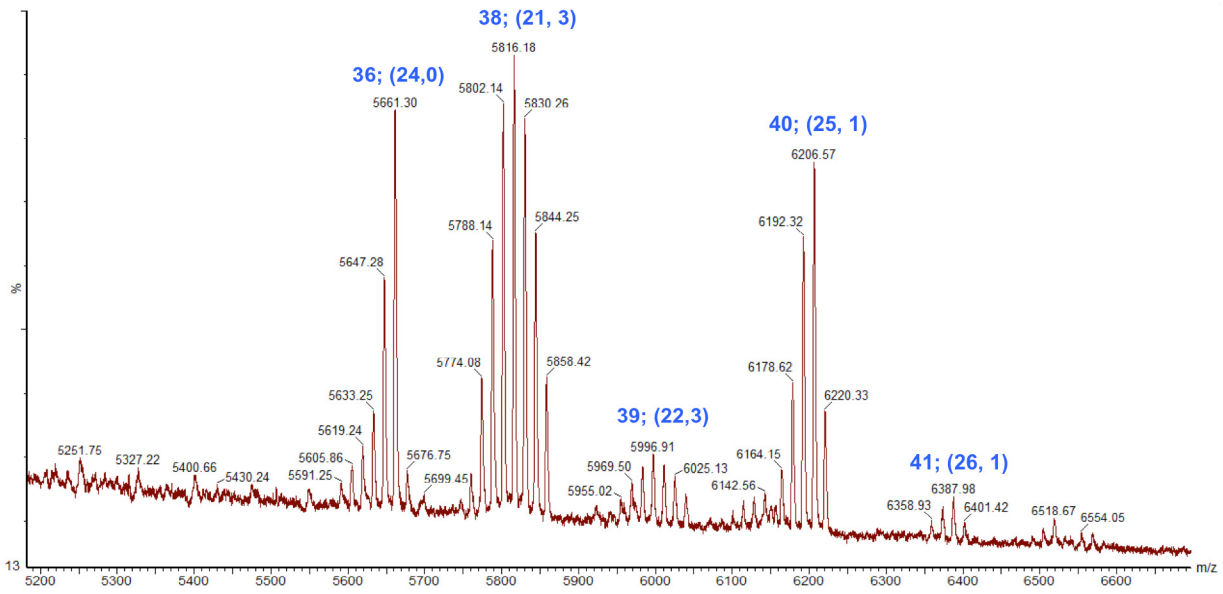

Figure S2. Zoom-inESI-MS spectrum of the 35 min sample. Small amounts of $Au_{39}(SR)_{25}$ and $Au_{41}(SR)_{27}$ were observed together with the three intense sets of $Au_{36}(SR)_{24}$, $Au_{38}(SR)_{24}$ and $Au_{40}(SR)_{24}$. The numbers of [n;(x, y)] on the top of peaks indicate $Au_n(TBBT)_x(PET)_y$.

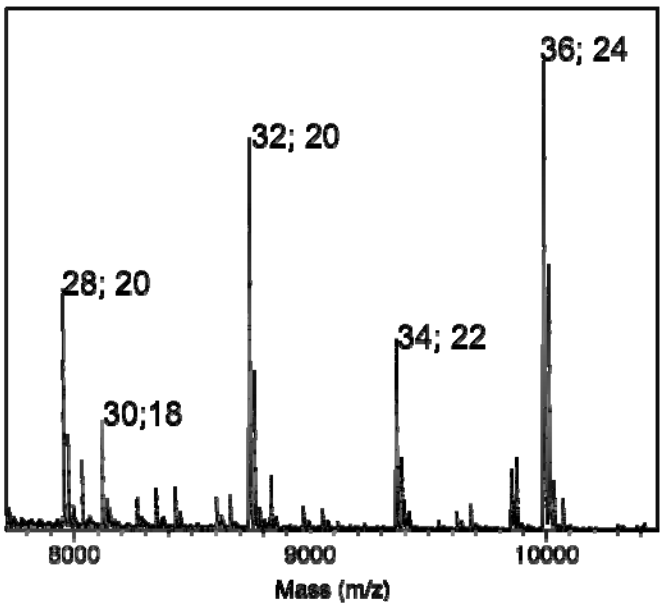

Figure S3. ESI-MS of the final product of Au_{38} reacting with cyclohexanethiol. A mixture of nanoclusters were observed (as opposed to clean $Au_{36}(TBBT)_{24}$ in the reaction with TBBT). The numbers in the form of (n; m) indicates $Au_n(SC_6H_{11})_m$.

Kinetics for stage II and III. In stage II, when more and more PET are exchanged by TBBT, the original rod-like Au_{38} structure becomes a distorted structure (denoted as Au_{38}*). This process causes the significant increase in absorbance (A) at 550 nm due to the difference in the extinction coefficient (ε) between Au_{38} and Au_{38}* at this wavelength. For Au_{38}, $\varepsilon_{Au_{38}}$ at 550 nm is measured to be 49,718 M^{-1} cm^{-1}, while for Au_{38}*, $\varepsilon_{Au_{38}*}$ is calculated to be 67,580 M^{-1} cm^{-1} by assuming that at the maximum absorbance (A_{max} at 550 nm), all the Au_{38}nanoclusters are converted to the Au_{38*} form (i.e. $A_{\max} = \varepsilon_{Au_{38*}} c_{Au_{38,0}}$); hence, the concentration of Au_{38} ($c_{Au_{38}}$) at different time can be roughly determined by equ. (1) based on the change of absorbance (A) at 550 nm ($A = \varepsilon_{Au_{38}} c_{Au_{38}} + \varepsilon_{Au_{38*}} c_{Au_{38*}}$).

$$Au_{38} \xrightarrow[TBBT]{k_2} Au_{38*}$$

$$c_{Au_{38}} = \frac{A - A_{\max}}{\varepsilon_{Au_{38}} - \varepsilon_{Au_{38*}}} \quad \text{.....(1)}$$

$$-dc_{Au_{38}} / dt = k_{2,obs}[c_{Au_{38}}]^n \quad \text{.....(2)}$$

Since the concentration of TBBT is around 4000 times higher than Au_{38}, the rate law can be simplified as equation (2), where $k_{2,obs}$ is the observed rate constant for stage II. In order to determine the reaction order, we measured the kinetic curves at different starting Au_{38} concentrations while keeping other conditions the same (Figure S4). It was found that the time for the 550 nm peak to reach the maximum is independent of the starting Au_{38} concentration, hence it is a first-order reaction (for first-order reactions, $t_{1/2} = (\ln 2)/k$, independent of $c_{Au_{38}}$). Then we plotted $\ln(c_{Au_{38}})$ against t, and a linear fitting was applied from t = 200 to 600 s (Figure S5A). When t < 200s, the data exhibits fluctuations due to the turbulence when the solution was heated from R.T. to 80 °C, hence the initial data points are excluded from the fitting. When t > ~600s, the overlap between stage II and stage III also makes the data less independent and hence these data points are excluded from fitting. The obtained rate constant for stage II at 80 °C is $k_{2,obs} = 3.5 \times 10^{-3} (s^{-1})$. The $k_{2,obs}$ at different temperatures are calculated in a similar way, and the results are summarized in Table 1 (main text).

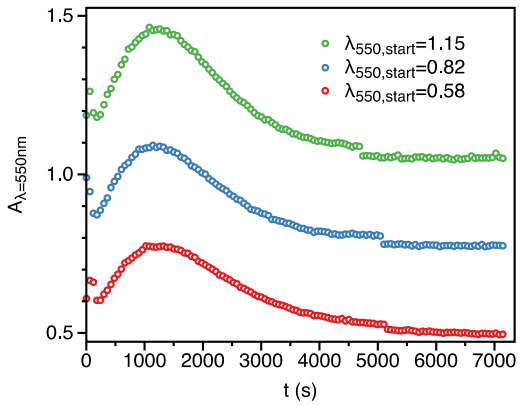

Figure S4. Kinetic curves for different starting concentrations of Au_{38}. Reaction was done at 80 °C, with 10 µl TBBT in 1ml toluene.

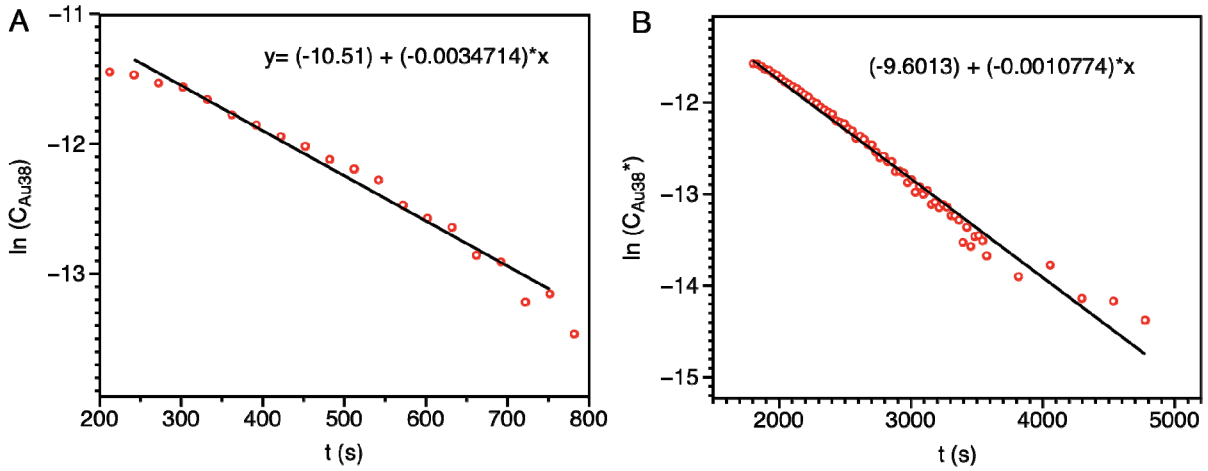

Figure S5. First-order fitting of the kinetic data for stage II (A) and stage III (B) at 80 ^{o}C.

A similar method was used to obtain the rate constant of stage III. In stage III, the absorbance at 550 nm is contributed by Au_{38}*, Au_{36} and Au_{40}. Several assumptions are made to obtain the concentration of Au_{38}* at different time: (i) The starting point of stage III is set at the point when $A_{\lambda 550}$ reaches the maximum, and the ending point is set at when the characteristic peak of Au_{38}* at ~805 nm disappears (Figure 1); (ii) At the starting point, all the absorbance is attributed to Au_{38}*, while at the ending point the absorbance is contributed by Au_{36} and Au_{40}; (iii) The concentrations of Au_{36} and Au_{40} are the same during stage III. Hence the mixed extinction coefficient, ε_{36+40}, is calculated to be 41,431 M^{-1} cm^{-1}. The concentration of Au_{38}* at different times is then determined based on eq. (3). The first-order kinetic model is also used to obtain the rate constant of stage III. Figure S5B shows the linear fitting of $\ln(c_{Au38}*)$ *vs* *t*, and the rate constant is determined to be $k_{3,obs} = 1.1 \times 10^{-3} (s^{-1})$. The rate constants at other temperatures are similarly obtained and summarized in Table 1 (main text).

$$Au_{38*} \xrightarrow[TBBT]{k_3} Au_{36} + Au_{40}$$

$$c_{Au_{38*}} = \frac{A - A_{final}}{\varepsilon_{Au_{38*}} - \varepsilon_{Au_{(36+40)}}} \quad \text{.....(3)}$$

$$-dc_{Au_{38*}} / dt = k_{3,obs}[c_{Au_{38*}}]^n \quad \text{.....(4)}$$

With the obtained rate constants at different temperatures (60, 70, and 80 ^{o}C), the activation energy (E_a) is obtained by plotting $\ln(k)$ against $1/T$ (Figure S6). For stage II, $E_{a,II}$ is ~107 kJ/mol. For stage III, $E_{a,III}$ is ~152 kJ/mol.

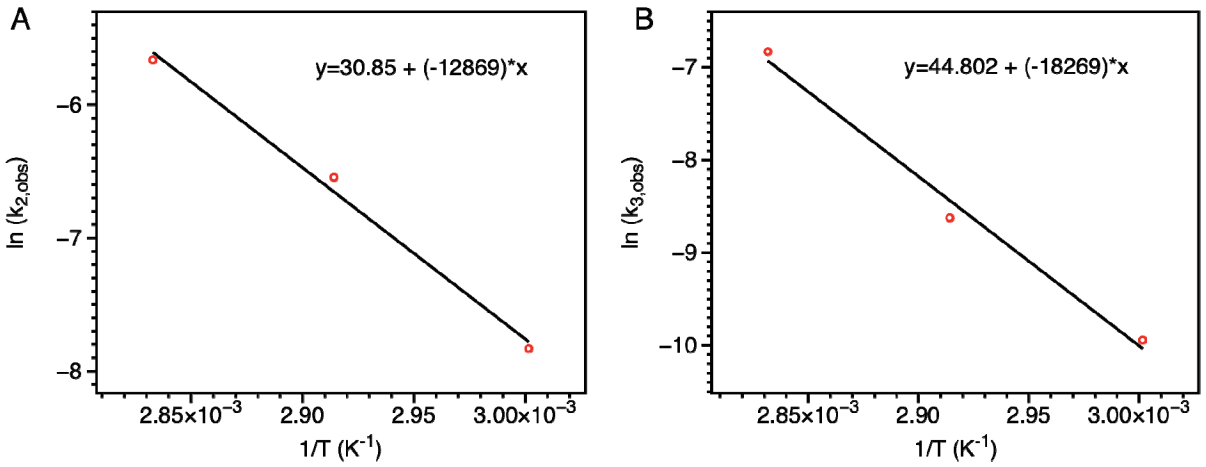

Figure S6. Determination of the activation energies for stage II (A) and III (B) by plotting ln(k) vs. $1/T$.